REACTION AND SINTERING OF $(Ni,Mg)(Al,Fe)_2O_4$ MATERIALS AND THEIR CORROSION PROCESS IN Na_3AlF_6-AlF_3-K_3AlF_6 ELECTROLYTE

Yibiao Xu*, Yawei Li, Jianhong Yang, Shaobai Sang

The State Key Laboratory of Refractories and Metallurgy, Wuhan University of Science and Technology, Wuhan, PR China

xuyibiao@wust.edu.cn

ABSTRACT

New types of refractory materials need to be developed for designing the so-called ledge-free sidewalls of the Hall-Héroult cell, which are currently constructed using Si_3N_4 bonded SiC refractories. In the present paper, $(Ni,Mg)(Al,Fe)_2O_4$ materials were prepared using fused magnesia, reactive alumina, nickel oxide and iron oxide powders. The sintering behaviors of specimens and their corrosion resistance to molten electrolyte have been investigated. The results show that after firing at temperature ranging from 1400°C up to 1600°C, all specimens prepared are composed of single-phase $(Ni,Mg)(Al,Fe)_2O_4$ composite spinel, whose lattice parameter increases with increasing Fe^{3+} ion concentration. Increasing the iron oxide content enhances densification of the specimens, which is accompanied by the formation of homogeneously distributed smaller pores in the matrix. The corrosion tests show that corrosion layers consist of fluoride and $Ni(Al,Fe)_2O_4$ composite spinel grains are produced in specimens with Fe/Al mole ratio no more than 1, whereas dense $Ni(Al,Fe)_2O_4$ layers are formed on the surface of the specimens with Fe/Al mole ratio more than 1. The dense $Ni(Al,Fe)_2O_4$ composite spinel layers formed improve the corrosion resistance of the specimens by inhibiting infiltration of electrolyte and hindering chemical reaction between the specimen and electrolyte.

INTRODUCTION

Si_3N_4 bonded SiC refractories have been currently widely used as sidewall materials in aluminum reduction cell because of their excellent properties such as high corrosion resistance to electrolyte, good thermal shock resistance and high thermal conductivity [1]. In practice, due to rapid heat dissipation through sidewalls, a layer of solidified electrolyte normally termed side ledge forms on the sidewalls, which protects the sidewalls from a corrosive electrolyte [2]. For this ledge to form and be stable, a large amount of heat accounting for approximately 35% of total energy consumption has to transfer [3]. To conserve the heat, high insulation layers could be applied outside the sidewalls [4]. In this case, however, the sidewalls could be in direct contact with oxidizing gas and corrosive electrolyte since the frozen ledge would no longer be existent. At the bath/gas interface, the Si_3N_4 bonded SiC sidewalls would be significantly corroded owing to combination attack of both oxidizing gas and corrosive electrolyte [1]. Therefore, new types of sidewall materials with higher resistance to oxidation and electrolyte are required within ledge free cell.

$NiFe_2O_4$ ceramic has been considered as the most promising inert anode due to its high stability in air and molten electrolyte [5]. Since the desirable properties of sidewall materials are quite similar to that proposed for inert anodes, $NiFe_2O_4$ is of interest as novel sidewall materials [6]. However, the possibility of aluminum contamination because of preferential dissolution of Fe and the high manufacturing costs due to scarcity of Ni resources eliminate the possibility of wide use of pure $NiFe_2O_4$ ceramics as sidewall materials [7]. In fact, the incorporation of other oxides to the spinels might improve their chemical stability by formation of composite spinel phases. For example, the $(Ni,Mg)Al_2O_4$ possessed better stability in the electrolyte than both $NiAl_2O_4$ and $MgAl_2O_4$ [3]. Thus, it can be predicted that the respective incorporation of MgO and Al_2O_3 to $NiFe_2O_4$ for partial substitution of NiO and Fe_2O_3 would increase the corrosion resistance of $NiFe_2O_4$ spinel. Besides, the manufacturing costs of the sidewalls and the risk of Al contamination can be reduced due to the decreased Ni and Fe content.

In the present work, we propose to prepare a series of $(Ni,Mg)(Al,Fe)_2O_4$ materials as candidate materials for use as sidewalls in ledge free cell using fused magnesia, reactive alumina, nickel oxide and ferric oxide powders. Firstly the phase evolutions and sintering behaviors of the selected mixtures are studied at high temperatures. Subsequently, a set of experimental results to demonstrate their chemical stabilities towards molten electrolyte are presented. Finally the electrolyte corrosion mechanism is proposed, taking into account the results of thermodynamic calculations.

EXPERIMENTAL

In this experiment fused magnesia (<0.045mm, 98

wt%MgO), nickel oxide (<0.045mm, 98 wt%NiO), ferric oxide (<0.045mm, 99 wt%Fe_2O_3) and reactive alumina (2μm, 99 wt% Al_2O_3) were used as raw materials. Seven groups of specimens were designed (Tab.1). After mixing the raw materials, specimens of 20 mm in diameter and 20 mm in height were prepared by cold pressing at a pressure of 120 MPa. All the specimens were fired at 1000-1600°C for soaking time of 3 h. After firing, the furnace was allowed to cool to room temperature.

Tab. 1: Batch compositions of the specimens.

specimens	Composites (mole fraction)			
	MgO	NiO	Al_2O_3	Fe_2O_3
F0	0.25	0.25	0.5	0
F1	0.25	0.25	0.45	0.05
F3	0.25	0.25	0.35	0.15
F5	0.25	0.25	0.25	0.25
F7	0.25	0.25	0.15	0.35
F9	0.25	0.25	0.05	0.45
F10	0.25	0.25	0	0.5

The bulk density and apparent porosity were determined by Archimedes principle. The phase composition was analysed by X-ray diffraction (XRD). The microstructures of specimens were analysed using scanning electron microscope (SEM) linked with energy dispersive spectroscopy (EDS) system. The corrosion test for all the specimens fired at 1600°C was conducted by immersing the specimens in a premixed Na_3AlF_6-AlF_3-K_3AlF_6 electrolyte in stainless steel crucibles. The crucibles were heated to 900°C and held at this temperature for 10 h. The chemical composition of the premixed electrolyte was 16.7Na_3AlF_6-25.5AlF_3-57.8K_3AlF_6 (wt%).

RESULTS AND DISCUSSION

In order to study the phase evolutions in the NiO-MgO-Al_2O_3-Fe_2O_3 system, specimen F5 was fired at 1000-1600°C and then analysed using XRD (Fig. 1(a)). It can be seen that the peak intensity of NiO, Fe_2O_3, periclase and corundum phases decreased with increasing temperature and was almost no longer observable after firing at temperatures higher than 1200°C. However, a (Ni,Mg)(Al,Fe)$_2O_4$ composite spinel phase appeared after firing at 1000°C whose content increased with firing temperature. After firing at 1400°C to 1600°C, only the (Ni,Mg)(Al,Fe)$_2O_4$ composite spinel phase was observed in specimen F5. For all the specimens fired at 1600°C, the presence of the peaks corresponding to the planes (311), (222), (400), (511) and (440) in the pattern reveals that all the specimens can be indexed as the single-phase cubic spinel structure (Fig. 1(b)). Similar to the previous research works [8], the crystal structure of the (Ni,Mg)(Al,Fe)$_2O_4$ varied with the chemical composition. The 2θ value of the (311) peak of (Ni,Mg)(Al,Fe)$_2O_4$ in specimens fired at 1600°C decreased with the increase in Fe_2O_3 content; it was 37.081, 36.816, 36.540, 36.226, 36.010, 35.757 and 35.619 in specimens of F0, 1, 3, 5, 7, 9 and 10, respectively (Fig. 2(a)). However, as shown in Fig. 2(b), as the firing temperature was higher than 1400°C, the 2θ value of (311) peak of the composite spinel in specimen F5 was almost unchanged.

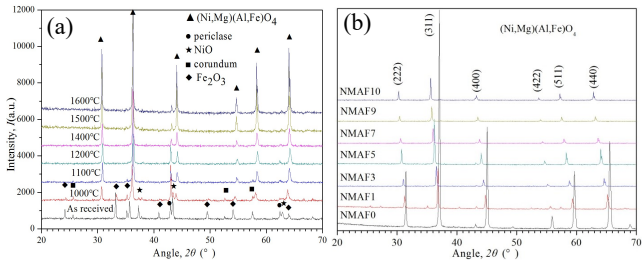

Fig. 1 XRD patterns of specimen F5 (a) and all specimens after firing at 1600°C (b).

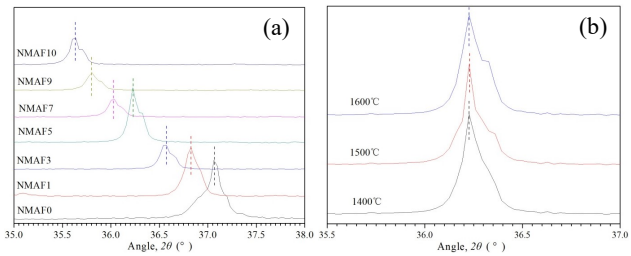

Fig. 2 XRD 2θ scans of specimens after firing at 1600°C (a) and specimen F5 after firing at 1400°C, 1500°C and 1600°C (b).

The bulk density and apparent porosity of the specimens fired at various temperatures are illustrated in Fig. 3. The bulk density increased and apparent porosity decreased for the specimens fired at all temperatures studied when Fe_2O_3 was added. Specimens fired at higher temperatures showed higher bulk density and lower apparent porosity. The SEM micrographs of specimens fired at 1600°C (Fig. 4) also indicated that specimens with higher Fe_2O_3 content can be observed with formation of homogeneously distributed smaller pores in the matrix.

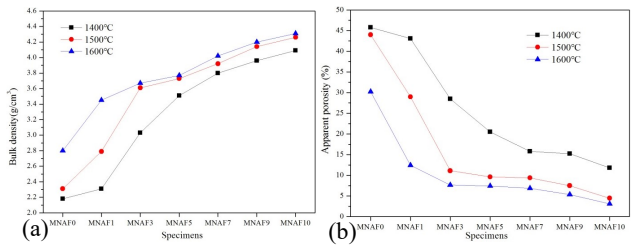

Fig. 3 Bulk density (a) and apparent porosity (b) of specimens.

The appearances of all specimens corroded by electrolyte are shown in Fig. 5. It can be seen clearly that the structure became

loose and big cracks formed on the surface of specimen F0. Additionally, some apparent cracks formed on the surface of specimen F1. No visible appearance change occurred in the rest of the specimens. The average thickness of corrosion layers are listed in Tab.2. Specimen F0 was damaged completely with a corrosion layer throughout the specimen. The corrosion layer thickness on specimen F1 was 2200 μm and decreased to 1200μm, 700μm, 120μm, 110μm and 80μm on specimens F3, 5, 7, 9 and 10, respectively, indicating that corrosion resistance of the specimens increased with increasing Fe_2O_3 content.

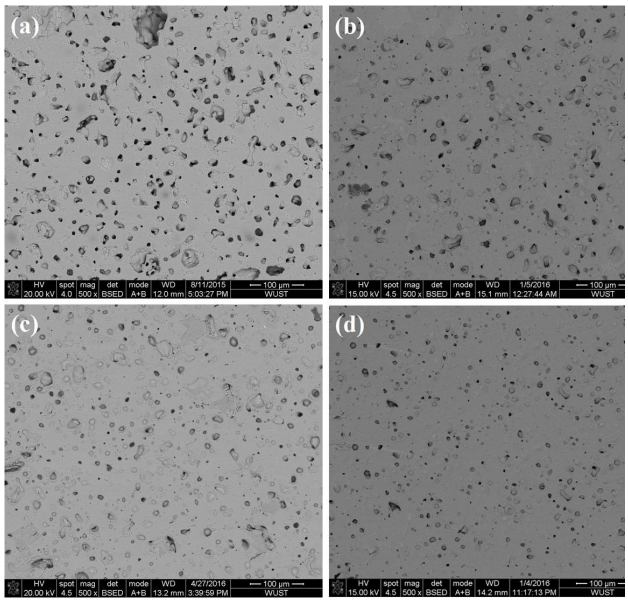

Fig. 4 SEM micrographs of specimens F1 (a), F5 (b), F7 (c) and F10 (d).

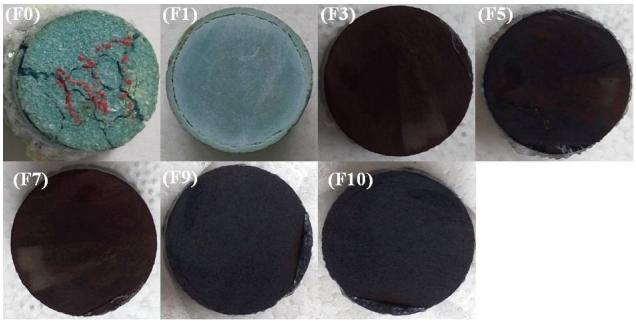

Fig. 5 The photos of the specimens after corroded by electrolyte.

Tab. 2 Average thickness of the corrosion layer for the specimens fired at 1600°C in molten electrolyte.

Thickness (μm)	Specimens						
	F0	F1	F3	F5	F7	F9	F10
Corrosion layer	Damaged	2200	1200	700	120	110	80

The SEM micrographs of the polished surface of the specimens after corrosion test are shown in Fig.6. The EDS analysis confirmed that the corrosion layer (C) in specimens F1, 3 and 5 was composed of $Ni(Al,Fe)_2O_4$ (bright white) and fluorides (dark gray). The amount of $Ni(Al,Fe)_2O_4$ increased and fluorides content decreased with the increase of Fe_2O_3. However, for specimens F7, 9 and 10, a dense layer (D) containing only $Ni(Al,Fe)_2O_4$ was formed on their surface. This layer could be regarded as the corrosion layer and it was even much denser than the $(Ni,Mg)(Al,Fe)_2O_4$ specimens themselves.

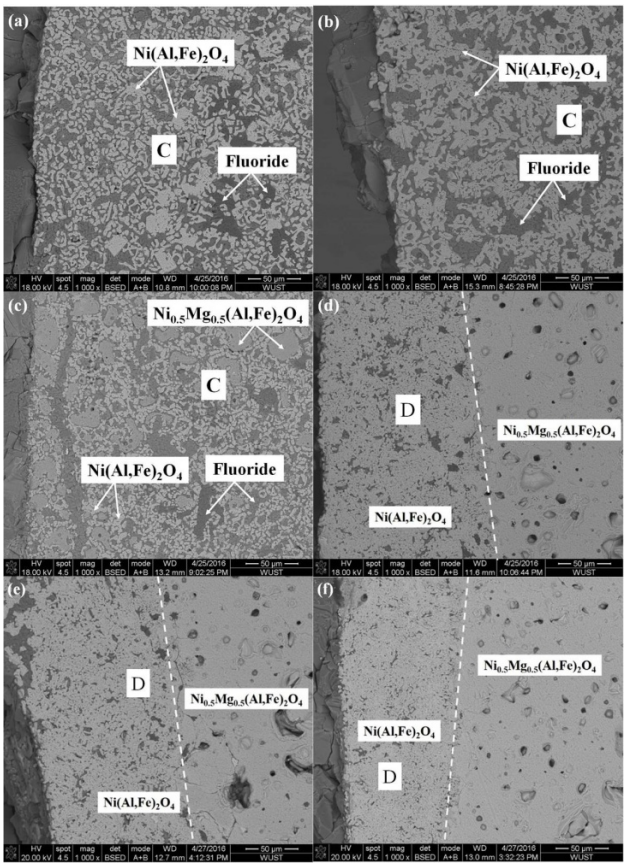

Fig. 6 SEM images of corroded surfaces of specimens F1(a), F3(b), F5(c), F7(d), F9(e) and F10(f).

In order to investigate the corrosion process and understand formation mechanisms of the $Ni(Al,Fe)_2O_4$ dense layers, phase evolution processes of specimen F7 in the electrolyte was simulated using thermodynamic software FactSage 6.2. The calculations were performed at 900°C. And 100 g mixed electrolyte was selected as the original corrosion slag. Alpha was defined as the weight ratio of specimen to electrolyte.

The predicted results (Fig. 7) indicate that the amounts of AlF_3 decrease with Alpha and drop to zero when Alpha reaches about 1.54. The content of K_3AlF_6 begins to decrease when alpha is 1.54 and reduces to zero as Alpha reaches about 2.74. However, the content of MgF_2 increases when Alpha value is lower than 1.54 and decreases thereafter. $KMgF_3$ and $NaMgF_3$ form when Alpha is 1.58 and 2.78, and their content increase after appearing. Moreover, $NiFe_2O_4$, $NiAl_2O_4$ and Al_2O_3 occur when Alpha is

greater than zero and their content increases successively with Alpha. Combining with EDS results and the thermodynamic calculation, the corrosion progresses of specimen F7 in electrolyte can be deduced as follows. During the corrosion test, after interaction between the specimen and electrolyte, NiO, Fe_2O_3, Al_2O_3 and the fluorides ($KMgF_3$, $NaMgF_3$ and MgF_2) would be produced via reactions (1)-(2). Followed by dissolutions of NiO, Fe_2O_3 and Al_2O_3 in the bath, $NiFe_2O_4$ and $NiAl_2O_4$ would be generated (reactions (3)) on the outer surface of the material [9]. The $NiAl_2O_4$ and $NiFe_2O_4$ phases have high chemical stability in molten electrolyte and can form $Ni(Al,Fe)_2O_4$ dense layer due to the same crystallographic structure[10]. The dense layer can improve the penetration and corrosion resistance of specimens by inhibiting infiltration of electrolyte. After test, no dense layer formed in specimens with Fe/Al mole ratio lower than 1, demonstrating that the presence of high Fe_2O_3 was favorable for formation of the dense layer.

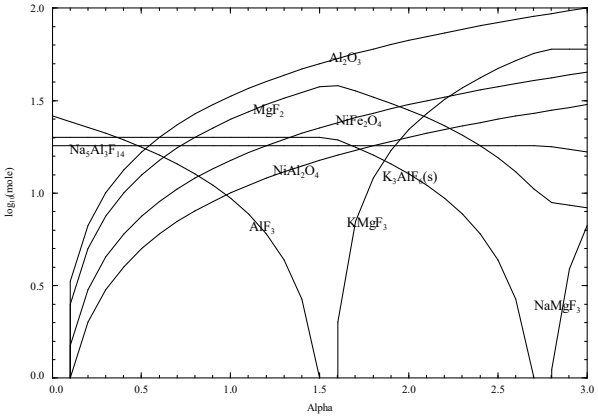

Fig. 7 Simulated phase evolution of the specimen F7 in the electrolyte at 900°C.

$$(Ni,Mg)(Al,Fe)_2O_4+AlF_3=NiO+MgF_2+Al_2O_3+Fe_2O_3 \quad (1)$$

$$2MgF_2+NaF+KF = NaMgF_3+ KMgF_3 \quad (2)$$

$$2NiO + Fe_2O_3 + Al_2O_3 = NiFe_2O_4 + NiAl_2O_4 \quad (3)$$

CONCLUSIONS

The following conclusions can be drawn by studying the sintering behavior of $(Ni,Mg)(Al,Fe)_2O_4$ materials and their corrosion resistance to molten electrolyte.

(1) A reaction sintering occurs in the NiO-MgO-Al_2O_3-Fe_2O_3 system in the range of 1000°C to 1200°C. After firing at 1400°C to 1600°C, all the specimens prepared are composed of single-phase $(Ni,Mg)(Al,Fe)_2O_4$ composite spinel, whose lattice parameter increases with increasing Fe^{3+} ion concentration. Increasing the iron oxide content enhances densification of the specimens, which is accompanied by the formation of homogeneously distributed smaller pores in the matrix.

(2) The corrosion tests show that corrosion layers consist of fluoride and $Ni(Al,Fe)_2O_4$ grains are produced in specimens with Fe/Al mole ratio lower than 1, whereas for specimens with Fe/Al mole ratio higher than 1, dense $Ni(Al,Fe)_2O_4$ corrosion layers are formed on their surface. This $Ni(Al,Fe)_2O_4$ composite spinel layers effectively improve the corrosion resistance of the specimens by inhibiting infiltration of electrolyte and hindering chemical reactions between the specimen and electrolyte. Therefore, the corrosion resistance of the specimens in the electrolyte increases progressively with the Fe_2O_3 content.

References

[1] Brooks G, Cooksey M, Wellwood G: Challenges in light metals production. Miner Process Extr Metall. 2007, 116: 25-33.

[2] Pan YH, Wright S, Sun S Y. Review and applications of thermal conductivity models to aluminium cell sidewall refractories. Int J Mod Phys B. 2012, 23: 790-795.

[3] Yan XY, Mukhlis RZ, Rhamdhani MA. Aluminate spinels as sidewall linings for aluminium smelters. Light Met. 2011: 1085-1090.

[4] Mukhlis RZ, Rhamdhani MA, Brooks G. Sidewall materials for Hall-Héroult process. Light Met. 2010: 883-888.

[5] Pawlek RP. Inert anode: Research, development, and potential. Light Met., 2002: 50-55.

[6] Nightingale SA, Longbottom RJ, Monaghan BJ. Corrosion of nickel ferrite refractory by Na_3AlF_6-AlF_3-CaF_2-Al_2O_3 bath. J Eur Ceram Soc. 2013, 33: 2761-2765.

[7] Sterten Å, Solli PA, Skybakmoen E. Influence of electrolyte impurities on current efficiency in aluminium electrolysis cells. J Appl Electrochem. 1998, 28: 781-789.

[8] Liu GP, Li N, Yan W. Composition and structure of a composite spinel made from magnesia and hercynite. J Ceram Process Res. 2012, 13: 480-485.

[9] Zhang L, Jiao WL, Yao GC. Prepation of $NiFe_2O_4$ inert anode and its electrolysis corrosion mechanism. J Eur Ceram Soc. 2005, 33: 1431-1436.

[10] Liu BG, Zhang L, Zhou KH. Electrical conductivity and molten salt corrosion behavior of spinel nickel ferrite. Solid State Sci. 2011, 13: 1483-1487.